Synchrotron Photoionization Mass Spectrometry Measurements of Kinetics and Product Formation in the Allyl Radical (H_2CCHCH_2) Self-Reaction[†]

Talitha M. Selby,[‡] Giovanni Meloni,[‡] Fabien Goulay,[§] Stephen R. Leone,[§] Askar Fahr,[||] Craig A. Taatjes,[‡] and David L. Osborn*,[‡]

Sandia National Laboratories, Combustion Research Facility, MS 9055, Livermore, California 94551-0969, Chemical Sciences Division, Lawrence Berkeley National Laboratory, Berkeley, California 94720, and Department of Chemistry, Howard University, Washington, D.C. 20059

Received: March 17, 2008; Revised Manuscript Received: June 26, 2008

Product channels for the self-reaction of the resonance-stabilized allyl radical, $C_3H_5 + C_3H_5$, have been studied with isomeric specificity at temperatures from 300−600 K and pressures from 1−6 Torr using time-resolved multiplexed photoionization mass spectrometry. Under these conditions 1,5-hexadiene was the only C_6H_{10} product isomer detected. The lack of isomerization of the C_6H_{10} product is in marked contrast to the C_6H_6 product in the related $C_3H_3 + C_3H_3$ reaction, and is due to the more saturated electronic structure of the C_6H_{10} system. The disproportionation product channel, yielding allene + propene, was also detected, with an upper limit on the branching fraction relative to recombination of 0.03. Analysis of the allyl radical decay at 298 K yielded a total rate coefficient of $(2.7 \pm 0.8) \times 10^{-11}$ cm^3 molecule^{-1} s^{-1}, in good agreement with previous experimental measurements using ultraviolet kinetic absorption spectroscopy and a recent theoretical determination using variable reaction coordinate transition state theory. This result provides independent indirect support for the literature value of the allyl radical ultraviolet absorption cross-section near 223 nm.

Introduction

An accurate assessment of the reaction kinetics and product channels of hydrocarbon radicals is central to the understanding of reaction systems such as those of combustion[1−3] and planetary atmospheres.[4,5] Small unsaturated hydrocarbon radicals, and in particular resonance-stabilized radicals, are believed to play crucial roles in combustion chemistry, producing polycyclic aromatic hydrocarbons that lead to soot formation.[1−3] These free radicals are postulated to play similar roles in planetary atmospheres.[4] Radicals with resonance structures can be produced abundantly in the gas phase as combustion intermediates, and via photolysis of hydrocarbons in planetary atmospheres. Because of their increased thermodynamic stability, resonance-stabilized radicals react more slowly with closed-shell molecules and attain higher concentrations than similar radicals lacking resonance stabilization. Consequently, reactions with atomic and molecular radical species are expected to be the dominant removal processes for resonance-stabilized radicals. Also the ability of resonance-stabilized hydrocarbon radicals to react with each other to form aromatic rings makes them key players in molecular weight growth chemistry.

Propargyl ($HCCCH_2$) and allyl (H_2CCHCH_2) radicals are two smaller and important examples of resonance-stabilized radicals. In recent years, substantial progress has been made in understanding the reaction kinetics and product channels of propargyl radicals.[6−10] A number of experimental[7−9] and computational studies[6,10] have reported propargyl self-reaction rate coefficients and detailed temperature and pressure dependent product branching fractions. These results demonstrate the significance of propargyl radicals as the most important precursor to the formation of the initial ring-containing hydrocarbons in flames, particularly benzene, dimethylenecyclobutene, fulvene, and phenyl radicals.[6−8]

The allyl radical is also an important intermediate in hydrocarbon reaction systems and its production and destruction schemes have been included in combustion and planetary atmospheric models. There are a limited number of reported studies on spectroscopy and reaction kinetics of the allyl radical

$$C_3H_5 + C_3H_5 \rightarrow \text{products} \qquad (1)$$

To date, all the measurements of the rate coefficient, k_1, have utilized absorption spectroscopy to monitor the concentration of allyl radicals. The experimental observable in such experiments is the ratio $k_1(T)/\sigma(\lambda,T)$, where $\sigma(\lambda,T)$ is the wavelength- and temperature-dependent absorption cross-section (base e) of the allyl radical. In 1982 Tulloch and co-workers[11] measured k_1/σ from 293 to 571 K using flash photolysis of 1,5-hexadiene as the allyl source, monitoring the allyl concentration via ultraviolet (UV) kinetic absorption spectroscopy at $\lambda = 223$ nm. They observed a slight negative temperature dependence, with $k_1/\sigma = (4.60 \pm 0.35) \times 10^5$ cm s^{-1} at 295 K. Their k_1/σ value was converted to $k_1(295\ \text{K}) = (2.65 \pm 0.2) \times 10^{-11}$ cm^3 molecule^{-1} s^{-1} using the allyl radical absorption cross-section $\sigma(\lambda = 223\ \text{nm}) = 5.7 \times 10^{-17}$ cm^2 molecule^{-1}, measured by van den Bergh and Callear in 1970.[12] Nakashima and Yoshihara measured time-resolved UV absorption spectra of allyl radicals following photolysis of allyl chloride at 193 nm.[13] Their measurements monitored the change in the absorption spectrum as the hot allyl photofragment cooled to equilibrium in collisions with 760 Torr of N_2 at 295 K. Although the integrated absorption coefficient for this electronic transition was nearly independent of internal excitation, the peak absorption cross-section increased from σ(220 nm, “hot”) = 3.64×10^{-17} to σ(223 nm, “relaxed”) = 7.73×10^{-17} cm^2 molecule^{-1}, implying that the allyl absorption cross-section decreases with increasing temperature.

[†] Part of the “Stephen R. Leone Festschrift”.

* Corresponding author. E-mail: dlosbor@sandia.gov.

[‡] Sandia National Laboratories.

[§] Lawrence Berkeley National Laboratory.

[||] Howard University.

10.1021/jp802330k CCC: $40.75

In 1993, Jenkin and co-workers[14] measured the allyl radical absorption cross-section from $\lambda = 210$ to 232.5 nm by photodissociating allyl iodide at $\lambda = 248$ nm, calibrating the allyl radical absorption to the photoinduced loss of allyl iodide. Using their allyl cross-section of $\sigma(220\text{ nm}) = (5.8 \pm 0.8) \times 10^{-17}$ cm^2 molecule^{-1}, they obtained $k_1 = (3.0 \pm 0.5) \times 10^{-11}$ cm^3 molecule^{-1} s^{-1} from a study of the 193 nm flash photolysis of 1,5-hexadiene. Boyd and co-workers[15] also used UV kinetic absorption spectroscopy, together with Jenkin et al.'s[14] $\sigma(220$ nm) value, to determine $k_1 = (2.6 \pm 0.2) \times 10^{-11}$ cm^3 molecule^{-1} s^{-1}, observing no temperature dependence of the rate coefficient from 403 − 540 K.

More recently, DeSain et al.[16] used the lowest-energy electronic transition, $\tilde{A}(^2B_1) \leftarrow \tilde{X}(^2A_2)$, to monitor allyl radicals, reporting an absorption cross-section of $(3.6 \pm 0.8) \times 10^{-19}$ cm^2 molecule^{-1} at $\lambda = 404$ nm. In that study 266 nm photolysis of allyl iodide was used to generate allyl radicals and I atoms. The allyl absorption cross-section at 404 nm was derived on the basis of comparison with the known I atom absorption cross-section at 1315 nm.[17] The allyl cross-section value reported by DeSain et al.[16] appears to be in significant disagreement with the value $\sigma(402.9\text{ nm}) = (2.0 \pm 0.4) \times 10^{-19}$ cm^2 molecule^{-1} of Tonokura and Koshi.[18] Although the discrepancy between these two values may be due to the different spectral characteristics of the lasers used, Tonokura and Koshi's measurement uses the values of k_1 from Tulloch and Jenkin to derive the allyl radical concentration and hence links potential errors between the kinetics and absorption cross-section determinations in both electronic bands. In the most recent experimental work, Ismail and co-workers[19] reported an upper bound to the allyl recombination rate coefficient of $k_1 \leq (4.3 \pm 0.7) \times 10^{-11}$ cm^3 molecule^{-1} s^{-1} at 298 K based on allyl radical absorption cross-sections of $(1.8 \pm 0.3) \times 10^{-19}$ and $(4.2 \pm 0.5) \times 10^{-19}$ cm^2 molecule^{-1} at 404 and 408 nm, respectively. Georgievskii and co-workers[20] have recently calculated the allyl recombination rate coefficient to be 3.5×10^{-11} cm^3 molecule^{-1} s^{-1} at 298 K using variable reaction coordinate transition state theory. Their calculations also predict a negative temperature dependence of the rate coefficient.

These discrepancies in the rate coefficient k_1 argue for further experiments using methods that do not rely on optical absorption cross-sections. In addition, there is only a single study by James and Kambanis[21] on the product channels for allyl radical self-reaction, determined using end-product analysis via distillation and gas chromatography. In that study, allyl radicals were produced from the pyrolysis of diallyl oxalate. They concluded that 1,5-hexadiene is the only isomer of C_6H_{10} produced in the recombination of allyl radicals (1a) from 303 − 463 K, and the ratio of disproportionation (1b) to recombination (1a) under these conditions is $k_{1b}/k_{1a} = 0.008 \pm 0.001$.

$$C_3H_5 + C_3H_5 \rightarrow C_6H_{10}\ (\text{1,5-hexadiene}) \qquad \Delta H^\circ_{298} = -62\ \text{kcal/mol}^{22} \quad (1a)$$

$$\rightarrow C_3H_4 + C_3H_6 \qquad \Delta H^\circ_{298} = -32\ \text{kcal/mol}^{22,23} \quad (1b)$$

In this work, we measure the rate coefficient and product channels of the allyl radical self-reaction with a method that does not rely on the accuracy of optical absorption cross-sections. We employ time-resolved photoionization mass spectrometry for the simultaneous detection of the decay of allyl radical and the rise of reaction products with isomeric selectivity.

Experiment

These experiments were performed at the Chemical Dynamics Beamline of the Advanced Light Source (ALS) Synchrotron at Lawrence Berkeley National Laboratory using a side-sampled slow-flow reactor coupled to a multiplexed photoionization mass spectrometer. Neutral species, sampled from the flow reactor in real time, are ionized by continuously tunable vacuum ultraviolet synchrotron radiation with energies spanning 8.0−10.8 eV. Photoionization with a high-brightness synchrotron source provides a sensitive and selective detection method. Isomeric selectivity arises from the fact that different structural isomers of the same chemical formula generally have photoionization efficiency (PIE) spectra with different thresholds (ionization energies, IE), shapes (determined by the Franck−Condon overlap between neutral and cation), and intensities (determined by the electronic transition dipole moment).

The experimental apparatus has been described previously[24−26] and is used for both product identification and reaction kinetics studies. Briefly, for product identification studies, allyl radicals were produced from the photodissociation of allyl bromide (Aldrich, 99% purity) at 248 nm using a KrF excimer laser (∼15 mJ cm^{-2} pulse^{-1}). The photodissociation laser beam propagates down the reactor, a 62 cm long quartz tube with 1.05 cm inner diameter, wrapped with nichrome heating tape. Gases are sampled through a 650 μm pinhole in the side of the reactor, forming a molecular beam that is skimmed and crossed with VUV radiation. The data were taken using an allyl bromide concentration of $\sim 2 \times 10^{13}$ molecules cm^{-3}, in a buffer gas of helium. The total molecular density was varied between $\sim 3 \times 10^{16}$ and 2×10^{17} molecules cm^{-3} by adjusting the flow rate of He and the pumping speed of the Roots blower connected to the slow-flow reactor. For product identification, the temperature was varied from 300 to 600 K, extending the range of James and Kambanis' work.[21] The flow velocity in the reactor was kept constant at ∼4 m s^{-1}. All species were monitored simultaneously using a Mattauch−Herzog geometry double-focusing sector mass spectrometer coupled to a time- and position-sensitive microchannel plate detector, covering a mass range of 13−130 amu. Time-dependent, multiplexed mass spectra were recorded as a function of photoionization photon energy. In this manner, a data set of 3-dimensional (3D) time- and energy-resolved mass spectra[27] was obtained at various temperatures and pressures. Because there was no observable dependence of the observed products with changes in temperature or pressure, these spectra could be coadded to improve the signal-to-noise ratio.

To probe isomer distributions in reaction 1, photoionization efficiency curves of several pure C_6H_{10} isomers were acquired for comparison to the experimental PIE curves from the allyl + allyl reaction. Absolute photoionization cross-sections of the C_6H_{10} isomers were obtained by adding a known amount of propene, which has a known cross-section,[28] to standard samples of C_6H_{10} isomers.

As in previous studies,[14] we found that allyl halide (C_3H_5X; X = Cl, Br, I) precursors, although intense and generally clean sources of allyl radicals, complicate determinations of reaction kinetics due to the fast, second-order competing reaction

$$C_3H_5 + X \rightarrow C_3H_5X \qquad (2)$$

Jenkins et al.[14] measured $k_2 = (16 \pm 6) \times 10^{-11}$ cm^3 molecule^{-1} s^{-1} for the allyl + iodine atom reaction, approximately a factor of 6 larger than the expected allyl self-reaction rate. Our experiments using allyl chloride and bromide precursors are consistent with similarly large values of k_2 for these halogen

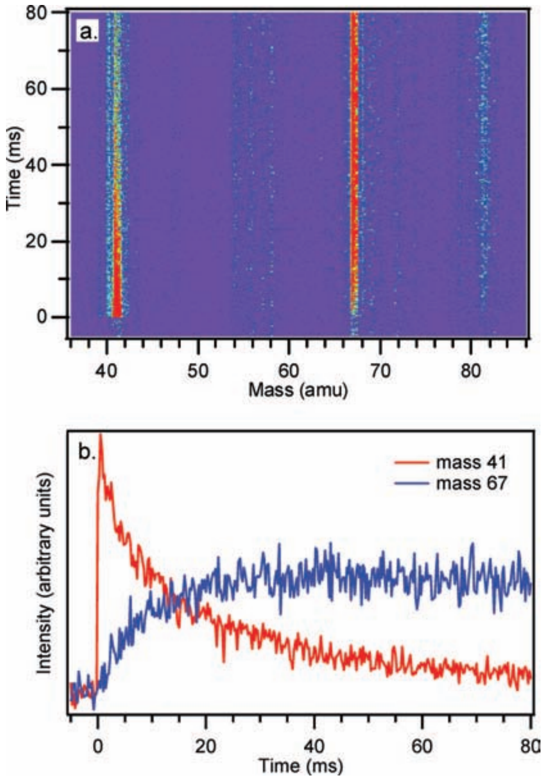

Figure 1. (a) Time-resolved mass spectrum resulting from the 248 nm photodissociation of allyl bromide integrated over photon energies 9.7−10.1 eV. (b) Time traces of masses 41 (C_3H_5) and 67 (C_5H_7) integrated over photon energies 9.7−10.1 eV. Mass 67 is a daughter ion of mass 82 (C_6H_{10}) and represents the time profile of C_6H_{10}.

atoms. Although the photodissociation of 1,5-hexadiene at λ = 193 nm is not as clean a source of allyl radicals as allyl halides (vide infra), it produces substantially lower densities of other free radicals that deplete the allyl radical pool, and we have used this precursor exclusively for allyl production in our determination of k_1. Although a reinvestigation of the temperature dependence of the allyl self-reaction is warranted,[20] such work is beyond the scope of the present experiments, where we have measured the value of k_1 only at 298 K.

Results and Discussion

A. Product Channels. Figure 1a shows the time-resolved mass spectrum resulting from the 248 nm photodissociation of allyl bromide in the range 35−85 amu. This spectrum was obtained by integrating over the photon energies between 9.7 and 10.1 eV. The two dominant signals are due to masses 41 (C_3H_5) and 67 (C_5H_7). Time profiles for these two species are shown in Figure 1b. Mass 41 (C_3H_5) shows an instrument-limited, fast rise time and slow decay, consistent with a prompt photodissociation to produce allyl radical, which then decays via reactions. At these photon energies, the C_6H_{10} product is most sensitively monitored via its daughter ion at mass 67 (C_5H_7). As shown in Figure 1b, the time trace of C_6H_{10} shows a slow rise, with a time-constant matching the C_3H_5 decay, consistent with product formation due to allyl radical recombination. Minor signals are also observed for masses 40 (C_3H_4), 42 (C_3H_6), 54 (C_4H_6), and 82 (C_6H_{10}). The time traces of masses 54 and 67 are identical to the mass 82 time trace, and all arise from dissociative ionization of mass 82 (C_6H_{10}). The time trace of mass 40 has a fast onset followed by nearly constant signal, consistent with a stable product formed by photodissociation. The time trace of mass 42 (after subtracting 3.2% of the mass 41 signal, representing C_3H_5 with a single ^{13}C substitution) has a slower onset, consistent with a slowly formed reaction product.

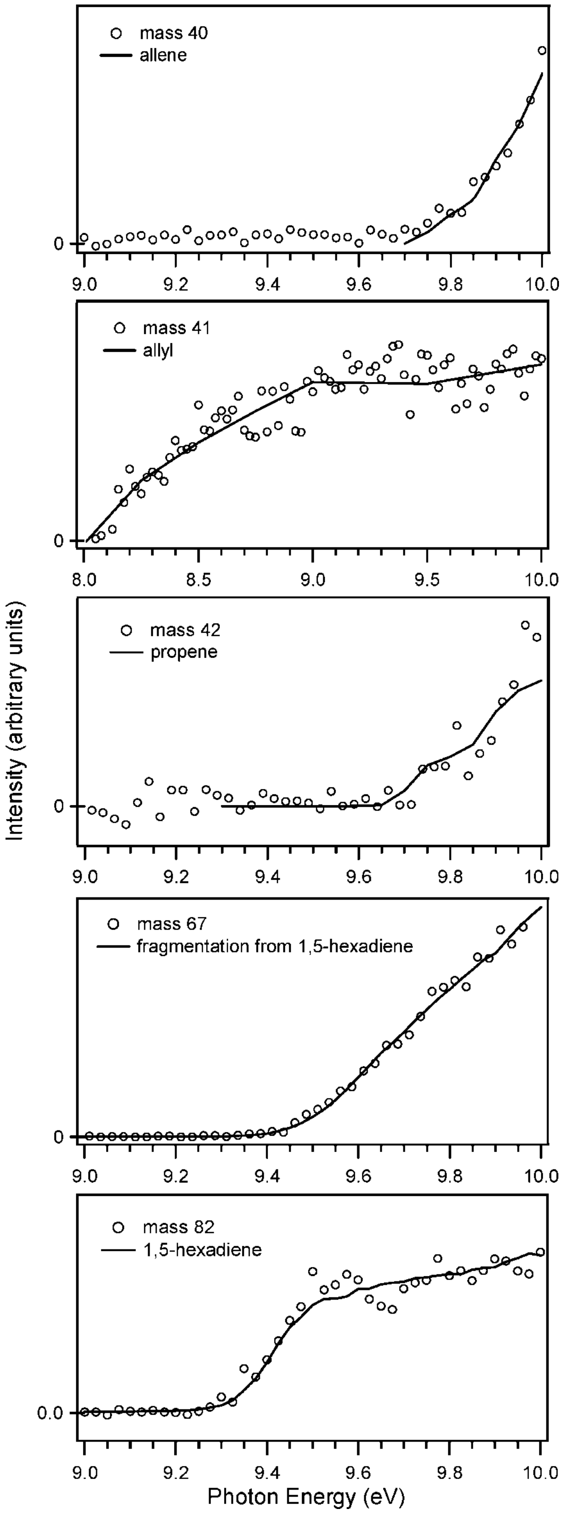

Figure 2. Experimental PIE curves (circles) resulting from the 248 nm photodissociation of allyl bromide integrated from 0 to 80 ms and reference PIE curves (solid lines) of allene, allyl, propene, and 1,5-hexadiene detected at two different masses.

To confirm the identity of each of the observed species, the 3D data were integrated over time (0−80 ms), normalized by the VUV photon flux, and background subtracted to produce photoionization efficiency scans of all masses. Figure 2 compares the time-integrated PIE scans at five different masses, resulting from allyl bromide photodissociation and subsequent reactions, to reference PIE spectra of specific isomers with the same mass. The PIE spectra of masses 40 (C_3H_4), 41 (C_3H_5), and 42 (C_3H_6) are assigned exclusively to the isomers allene,[28] allyl radical,[29] and propene,[28] respectively. The PIE spectrum of mass 82 (C_6H_{10}) is consistent with 1,5-hexadiene, and that of mass 67 (C_5H_7) is consistent with dissociative ionization of 1,5-hexadiene.[30]

Our simultaneous measurement of all products from the recombination channel (1a) and the disproportionation channel (1b) provides, in principle, a determination of the branching ratio k_{1b}/k_{1a}. In practice, this measurement is complicated by several factors. First, the measured densities of allene and propene are quite small compared to 1,5-hexadiene, implying that the recombination channel dominates. Over the range 1−6 Torr there is no dependence of the product yields on pressure. Second, the allene time profile rises promptly (within 0.25 ms) to an essentially constant value that is 4.6 times larger than the propene density at long time. On the basis of the allene time profile, we conclude that most of the allene arises from a minor photodissociation channel of allyl bromide at $\lambda = 248$ nm:

$$C_3H_5Br \rightarrow H_2CCCH_2 + HBr \qquad (\Delta H^\circ_{298} = 25.3 \text{ kcal/mol})^{22} \quad (3a)$$

Note that the probability of the three-body fragmentation

$$C_3H_5Br \rightarrow H_2CCCH_2 + H + Br \qquad (\Delta H^\circ_{298} = 113.2 \text{ kcal/mol})^{22} \quad (3b)$$

is almost certainly negligible in light of the minimal available energy for this channel given the 115.2 kcal/mol energy of a 248 nm photon. In contrast, the time profile of propene, within our signal-to-noise, has a risetime no faster, and perhaps slightly slower, than 1,5-hexadiene. The long time (50−80 ms) propene density can be adequately fit using a branching fraction $k_{1b}/k_{1a} = 0.085$. If this branching fraction were correct, the allene signal should show a similar slow-rise component from allene produced by disproportionation of two allyl radicals, built on top of the allene that is clearly produced by photodissociation of allyl bromide. The largest value of k_{1b}/k_{1a} that could be consistent with our constant (though somewhat noisy) postphotodissociation allene signal is $k_{1b}/k_{1a} = 0.03$. Therefore, we concluded that much of the weak, time-resolved propene signal we observe comes from a reaction other than (1b) and place an upper limit on the disproportionation to recombination ratio of $k_{1b}/k_{1a} \leq 0.03$.

Figure 3a presents absolute total photoionization cross-sections of the C_6H_{10} isomers 1,5-hexadiene, 2,4-hexadiene, 2,3-dimethyl-1,3-butadiene, 1,3-hexadiene, and 1,4-hexadiene, calibrated to the propene standard. Figure 3b shows the partial cross-section producing parent ions at mass 82. Partial ionization cross-sections of all fragments for these isomers are provided in the Supporting Information. The time-resolved PIE spectra of ions arising from the C_6H_{10} product in the allyl + allyl reaction are in excellent agreement with the reference 1,5-hexadiene PIE spectra at the parent and all daughter ion masses. Because 1,5-hexadiene has the highest ionization energy (9.27 eV) and the lowest partial ionization cross-section at mass 82 of the C_6H_{10} isomers listed above, we can confidently say that under the conditions of the present experiments less than 1% of the C_6H_{10} products are due to these other isomers. Cyclohexene and the methyl-substituted cyclopentene isomers of C_6H_{10} are more stable than the acyclic isomers listed above, but all have IEs below 9.0 eV and can be ruled out as reaction products at these temperatures.[22] Thus, if other C_6H_{10} isomers are present their concentrations (or, conceivably, their ionization cross-sections) must be extremely small. It should be noted that out of 58 possible C_6H_{10} structural isomers that have been previously observed,[22] 34 isomers can be strictly eliminated simply because their ionization energies lie below that of 1,5-hexadiene.

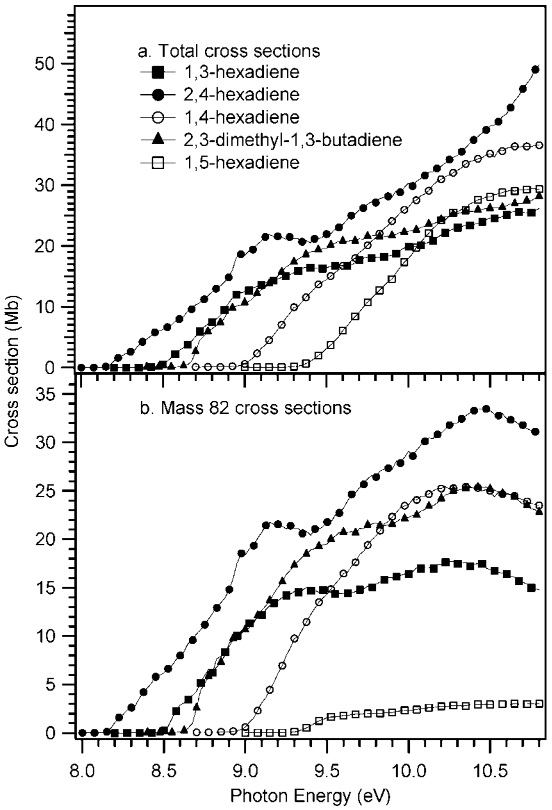

Figure 3. (a) Total photoionization cross-sections of several C_6H_{10} isomers. (b) Partial photoionization cross-sections of the mass 82 channel. Partial cross-sections of all fragmentation channels are provided in the Supporting Information.

The observation that the allyl + allyl reaction is dominated by stabilization to a single isomer, 1,5-hexadiene, with no observable isomerization to other C_6H_{10} isomers at temperatures up to 600 K, is in contrast to the substantial pressure and/or temperature effects on the product distributions that have been observed for the radical−radical reactions C_3H_3 + C_3H_3,[6,9,10] C_2H_3 + CH_3,[31,32] C_2H_3 + C_2H_3,[33] C_2H_3 + C_2H_5.[34] In general, the chemically activated adducts produced from these radical−radical reactions are either stabilized by nonreactive bimolecular collisions (at high pressures and/or low temperatures) or are subject to a variety of unimolecular reactions including isomerization, cyclization and decomposition (at low pressures and/or high temperatures). In the propargyl self-reaction, the initially formed linear C_6H_6 adducts isomerize via pericyclic reactions to other branched structures and efficiently cyclize to the ring-containing isomers dimethylenecyclobutene, fulvene, and benzene.[6,9,10]

In both propargyl and allyl radicals, unpaired electron density is concentrated at the terminal carbon atoms, creating two bonding sites. The CH_2 and CH ends of propargyl comprise two chemically distinct bonding sites, whereas allyl radical has a symmetric C_{2v} structure. Therefore, propargyl recombination leads to three possible initial C_6H_6 adducts, whereas allyl recombination leads to only one: 1,5-hexadiene. In addition, the degree of unsaturation of the 1,5-hexadiene adduct is lower than the C_6H_6 adducts from propargyl recombination. With only

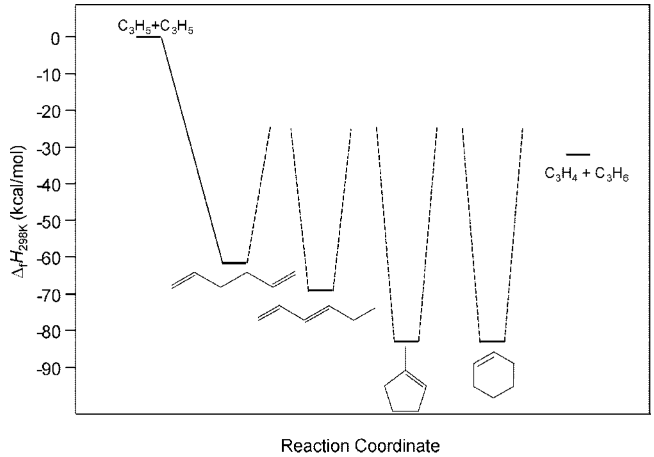

Figure 4. Relative enthalpies of several species on the C_6H_{10} potential energy surface. Heats of formation are obtained from ref 22.

TABLE 1: Quantum Yields from the 193 nm Photodissociation of 1,5-Hexadiene

product channel		quantum yield (%) this work[b,d]	quantum yield (%) Tulloch et al.[11]
methyl (CH_3)	+ C_5H_7	2.7	2.5
vinyl (C_2H_3)	+ C_4H_7[a]	2.1	0
ethene (C_2H_4)	+ 1,3-butadiene (C_4H_6)	2.3	2.5
cyclopropenylidene (C_3H_2)	+ C_3H_8[a]	3.1	0
allene (C_3H_4)[c]	+ propene (C_3H_6)	26.1	27
allyl (C_3H_5)	+ allyl (C_3H_5)	63.6	68
vinylacetylene (C_4H_4)	+ C_2H_6[a]	0.1	0

[a] This species was not observed. [b] To calculate the percent yield, the ionization cross-section of cyclopropenylidene was estimated to be 15 Mb at 10.8 eV. [c] The propene signal from this channel was used to determine the quantum yield. [d] There is ±15% error (1σ) associated with the quantum yields determined in this work.

two π bonds in acyclic C_6H_{10} versus four in acyclic C_6H_6, there are fewer opportunities to facilitate isomerization via uncoupling and recoupling of π bonds. Lastly, 1,5-hexadiene has 42 vibrational modes, compared to 30 in C_6H_6, and the resulting greater density of vibrational states leads to more efficient collisional stabilization at the expense of isomerization to more stable C_6H_{10} isomers. These characteristics vastly reduce the role of isomerization in allyl + allyl compared with the propargyl + propargyl system.

Figure 4 depicts the relative heats of formation of several C_6H_{10} isomers,[22] which allows a further discussion of the hindrance to isomerization in the allyl self-reaction. The 1,5-hexadiene adduct lies ~60 kcal/mol below the reactants and its formation is barrierless[20] similar to the $C_3H_3 + C_3H_3$ adducts.[20] The thermodynamics of C_6H_{10} favors isomerization to at least 14 lower energy isomers,[22] that are up to ~20 kcal/mol more stable than 1,5-hexadiene. Although the barriers for isomerization on the C_6H_{10} surface are not known, qualitative insight into the potential energy surface can be obtained by comparison to similar reactions. For example, on the C_6H_6 potential energy surface, all the transition states deemed relevant by Miller and Klippenstein[6] lie 25 kcal/mol or more below the reactant asymptote, and isomerization is facile in that system even though carbenes and strained bicyclic structures occur along the pathways to benzene. However, on the C_6H_6 surface, the most stable ring structures, fulvene and benzene, are ~40−70 kcal/mol more stable than the initial acyclic adducts, whereas on the C_6H_{10} potential energy surface, the most stable cyclic structures, cyclohexene and the methylcyclopentenes, are only ~20 kcal/mol more stable than the 1,5-hexadiene adduct. It is reasonable to assume that these much deeper wells on the C_6H_6 potential energy surface are concomitant with lower cyclization barriers compared to those on the C_6H_{10} potential energy surface. Therefore, we infer that the transition states connecting 1,5-hexadiene to the lower energy isomers in Figure 4 lie at energies greater than −25 kcal/mol with respect to reactants.

Thermochemical kinetic arguments[35,36] for individual potential isomerization pathways tend to corroborate this picture. For example, although the ring opening of cyclohexene has not been observed, the similar isomerization of cyclohexane to 1-hexene has an activation energy of 86 kcal/mol.[37] If the activation energy for cyclohexene is similar, this transition state would lie near the allyl + allyl energy (and well above the transition state for the reverse Diels−Alder reaction of cyclohexene to give ethene + 1,3-butadiene). Isomerization of 1,5-hexadiene to 1,4-hexadiene would proceed by a 1,3 hydrogen shift. The transition state for a Woodward−Hoffmann[38] allowed antarafacial 1,3 H-atom shift is typically similar in energy to the corresponding allylic radical + H atom,[39] i.e., on the order of 87 kcal/mol, placing it well above the allyl + allyl reactants. A 1,4 H atom shift in 1,5-hexadiene could form the same allylic biradical, $CH_3\dot{C}HCH_2\dot{C}HCH{=}CH_2 \leftrightarrow CH_3\dot{C}HCH_2CH{=}CH\dot{C}H_2$, which would result from simple 1,2 C−C bond homolysis in 1-methyl-2-vinylcyclopropane. The activation energy of the *trans*-1-methyl-2-vinylcyclopropane isomerization to 1,4-hexadiene (Δ_fH_{298} = 17.8 kcal/mol),[22] thought to proceed via such a C−C bond fission, is 48.6 kcal/mol.[40] Assuming the enthalpy of formation for the *trans*-1-methyl-2-vinylcyclopropane is similar to that of the *cis* isomer (Δ_fH_{298} = 24.7 kcal/mol),[22] the transition state for this isomerization would lie about 53 kcal/mol above 1,5-hexadiene (Δ_fH_{298} = 20.4 kcal/mol),[22] or ~9 kcal/mol below the allyl + allyl asymptote. The biradical formed via the other possible 1,4 hydrogen shift from 1,5-hexadiene, $CH_2\dot{C}CH_2CH_2CH_2\dot{C}H_2$, has no allylic resonance and should hence lie about 12 kcal/mol higher.[40] A 1,5 hydrogen shift in 1,5-hexadiene would produce a $CH_3\dot{C}HCH_2CH_2\dot{C}CH_2$ biradical that would presumably rapidly yield allene + propene products. Whereas pericyclic 1,5 H atom transfers have activation energies of around 35 kcal/mol,[35] the 1,5 H transfer in 1,5-hexadiene lacks extended π-conjugation and should be dramatically higher in energy. It is therefore reasonable that 1,5-hexadiene is the only isomer observed in allyl radical recombination under the present conditions given this sketch of the C_6H_{10} potential energy surface, coupled with the higher degree of saturation and greater vibrational state density of C_6H_{10} isomers compared to C_6H_6 isomers.

B. Kinetics. Simple second-order analysis of allyl decays using allyl bromide as the precursor gave an apparent rate coefficient about an order of magnitude larger than expected for the recombination of two resonance-stabilized radicals, likely because of the competing reaction of Br + C_3H_5. Similar results have been observed in other radical−radical reactions in the presence of a halide atom.[7,14] Therefore, to determine the recombination rate coefficient for allyl radicals, the 193 nm photolysis of 1,5-hexadiene was used as the allyl source. At this wavelength, Tulloch and co-workers[11] reported the photodissociation quantum yields for four dissociation channels given in Table 1.

Through analysis of the early time behavior of our time-resolved multiplexed mass spectra of 1,5-hexadiene photodissociation, we identified small amounts of vinyl (CH_2CH), cyclopropenylidene (c-C_3H_2), and vinylacetylene ($HCCCHCH_2$) and a significant amount of propargyl radical in addition to the

TABLE 2: Molecule Branching Fractions from 193 nm Photodissociation of 1,5-Hexadiene

species	branching fraction[a]
allyl (C_3H_5)	127.2 ± 19.1
propene (C_3H_6)	26.1 ± 3.9
propargyl (C_3H_3)	25.4 ± 3.8
allene (C_3H_4)	11.2 ± 1.7
cyclopropenylidene (c-C_3H_2)	3.1 ± 0.5
methyl (CH_3)	2.7 ± 0.4
ethene (C_2H_4)	2.3 ± 0.3
vinyl (CH_2CH)	2.1 ± 0.3
vinylacetylene ($HCCCHCH_2$)	0.10 ± 0.02

[a] Initial branching per 100 molecules of 1,5-hexadiene photodissociated.

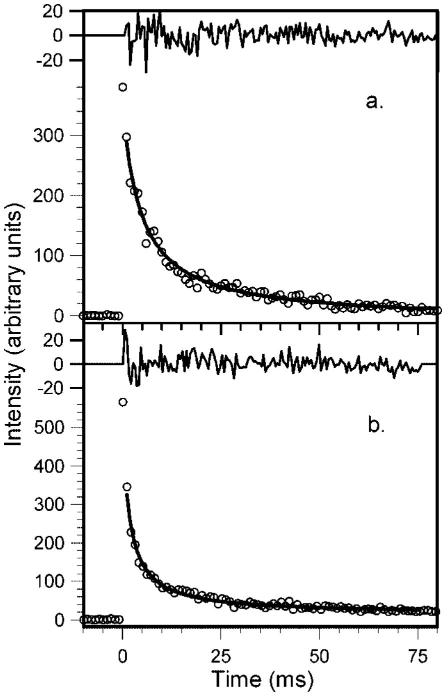

Figure 5. Allyl radical decay profiles (circles), together with fits and residuals from eq 4 for data recorded (a) at the ALS and (b) at Sandia. The initial concentrations of the allyl radicals are (a) 3.03 × 10^{12} and (b) 8.66 × 10^{12} molecules cm^{-3}.

photodissociation products observed by Tulloch and co-workers.[11] Initial concentrations of the photodissociation products were obtained by normalizing the observed signals (extrapolated to zero time as necessary) to the known photoionization cross-sections of each species at 10.8 eV[28,29,41−43] and our mass-dependent instrument response function.[44] An estimated cross-section[45,46] of 15 Mb was used for cyclopropenylidene, because its absolute photoionization efficiency has not been measured. The resulting photodissociation quantum yields, expressed as product channels, are compared to those of Tulloch et al. in Table 1. Because the propyl radical, the presumed dissociation partner of propargyl radical, was not observed, we ascribe the presence of propargyl to the dissociation of hot allene radicals. Thus, the propargyl radical is not included in Table 1 because it is not believed to be a primary photodissociation product. We observe less prompt allene than prompt propene, supporting this conclusion. Other unimolecular decay processes of internally excited primary photoproducts may also contribute, such as the decay of some allyl radicals to allene. Other than the presence of propargyl radicals, the photodissociation product channel results in this work are in good agreement with the results of Tulloch and co-workers.

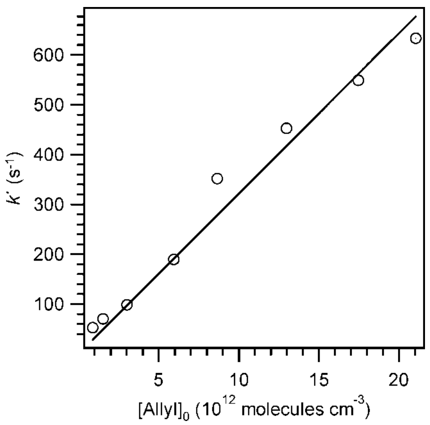

Figure 6. Plot of k' versus $[\text{allyl}]_0$.

Presenting the photodissociation products of 1,5-hexadiene as primary product channels (Table 1) is relevant for studying the photodissociation itself. For the purposes of studying the kinetics *following* 1,5-hexadiene photodissociation, branching fractions to each observed molecule, regardless of whether it is a primary or secondary product of photodissociation, are more relevant, because they directly provide the fractions of each species present before bimolecular reactions begin. Table 2 presents the number of molecules of each species observed per 100 molecules of 1,5-hexadiene dissociated.

To obtain the initial allyl concentration, a known concentration of 1,5-hexadiene (from 6.3 × 10^{12} to 9.7 × 10^{13} molecules cm^{-3}) in helium was photodissociated, and the percent depletion was recorded (11−17%). From the photodissociation quantum yields of 1,5-hexadiene, the initial allyl concentration was calculated as ranging from 8.8 × 10^{11} to 2.1 × 10^{13} (±15%) molecules cm^{-3}. The error associated with the initial allyl concentration is dominated by the error in the photodissociation quantum yields.

At the ALS, kinetic traces were averaged over several thousand laser shots using a single detection photon energy of 9.6 eV for photoionization of four different precursor concentrations. Later, four higher concentrations were studied at Sandia using a hydrogen hollow-cathode discharge lamp producing photons primarily at $h\nu = 10.2$ eV, equipped with a MgF_2 window to absorb higher energy photons. The resulting allyl decays were fit to a combined first- and second-order decay function, which considers only the allyl self-reaction and allyl wall loss. The following functional form was used:[47]

$$S(t) = \frac{S_0 k_{\text{wall}}}{(2k' + k_{\text{wall}})e^{k_{\text{wall}}t} - 2k'} + \text{baseline} \qquad (4)$$

where $k' = k_1[\text{allyl}]_0$, k_1 is the allyl self-reaction rate, $S(t)$ is the observed signal at time t, $S_0 \equiv S(0)$, and k_{wall} is the heterogeneous wall loss rate. For a photoionization energy of 9.6 eV, the signal returned to baseline at long time. However, at higher photon energies, a small offset at mass 41 was observed at long time and subtracted from the data. Possible sources of this baseline offset are dissociative ionization of a higher mass molecule and/or the large signals occurring at adjacent masses 40 and 42. Representative fits to the raw data for the allyl decay recorded at the ALS and at Sandia are shown in Figure 5a,b, respectively. After fitting the observed allyl signal at eight concentrations, a plot of k' versus $[\text{allyl}]_0$ was fit to a line with slope k_1, as shown in Figure 6. Using the photodissociation quantum yield of allyl determined in this work, k_1 was found to be (3.2 ± 1.0) × 10^{-11} cm^3 $molecule^{-1}$ s^{-1}, whereas using

TABLE 3: Kinetic Model Used To Determine the Allyl Self-Reaction Rate

reaction	rate coefficient
$C_3H_5 + C_3H_5 \rightarrow C_6H_{10}$	fit
$C_3H_3 + C_3H_3 \rightarrow C_6H_6$	3.90×10^{-11} (cm^3 molecule^{-1} s^{-1})[7]
$C_3H_3 + C_3H_5 \rightarrow$ products	7.50×10^{-11} (cm^3 molecule^{-1} s^{-1})[20]
C_3H_5 wall loss	13 (s^{-1})[a]
C_3H_3 wall loss	43 (s^{-1})[a]

[a] Determined from this work by fitting eq 4.

TABLE 4: Summary of Allyl + Allyl Rate Coefficients Determined near Room Temperature

group	$k_1/10^{-11}$ (cm^3 molecule^{-1} s^{-1})	temp (K)
Van den Bergh and Callear[12]	1.4 ± 0.5	298
Tulloch et al.[11]	2.65 ± 0.2	295
Jenkin et al.[14]	3.0 ± 0.5	296
Boyd et al.[15]	2.6 ± 0.2	403−540
Georgievskii et al.[20] (calculated)	3.5	298
Ismail et al.[19]	$\leq 4.3 \pm 0.7$	298
this work	2.7 ± 0.8	298

the photodissociation quantum yield of allyl from Tulloch's work yielded a rate coefficient of $(3.1 \pm 0.9) \times 10^{-11}$ cm^3 molecule^{-1} s^{-1}. The error bars for the rate coefficient represent 2 standard deviations. Because the statistical errors in the fits that determined the eight k' values plotted in Figure 6 were much smaller than the scatter in the data, we assume that most of the scatter is due to the uncertainty in the initial allyl concentration (±15% error, 1σ). Thus the reported 2σ uncertainty in k_1 is estimated directly from the error in the allyl concentration determination.

The above analysis assumes that the other radicals formed in the photodissociation of 1,5-hexadiene do not affect the observed allyl decay profile. However, this assumption cannot be valid with a relatively large amount of propargyl radical present (one for every five allyl radicals). To test our sensitivity to the presence of propargyl, the allyl time profile was fit using a five-reaction kinetic model detailed in Table 3. In this model the allyl self-reaction rate coefficient was fit, while the other reaction rate coefficients were fixed. This chemical mechanism should provide a more realistic description of the allyl radical decay profile, because it includes competing reactions. These fits produced a rate coefficient that was 1.17 ± 0.06 (1σ) times smaller than the rate coefficient from the simplified case where propargyl reactions were ignored. Using this correction, our best estimate for the allyl self-reaction rate is $k_1 = (2.7 \pm 0.8) \times 10^{-11}$ cm^3 molecule^{-1} s^{-1} at 298 K.

As summarized in Table 4, this result is in good agreement with previous measurements by Tulloch,[11] Jenkin,[14] and Boyd,[15] where the accuracy in k_1 depends on the accuracy of the UV absorption cross-section of allyl near 220 nm. Our measurement of k_1 by independent methods supports the absorption cross-section $\sigma(220-223 \text{ nm}) = 5.8 \times 10^{-17}$ cm^2 molecule^{-1} near room temperature. However, the UV absorption spectra of allyl from Nakashima and Yoshihara[13] offer clear evidence that this transition has a temperature-dependent cross-section, which must be considered in future kinetics measurements by this method at elevated temperatures. The recently determined theoretical value (3.5×10^{-11} cm^3 molecule^{-1} s^{-1}) of Georgievskii et al.[20] is 30% higher than our value, whereas the upper bound of Ismail et al.[19] is 59% larger. Our experiment is the first determination of the room temperature rate coefficient that does not rely on the optical absorption cross-section of the allyl radical.

Conclusions

We have measured the isomer-resolved product distribution of the allyl radical self-reaction using time-resolved photoionization mass spectrometry over the temperature range 300−600 K and pressure range of 1−6 Torr. 1,5-Hexadiene was the only isomer of C_6H_{10} detected, implying that the barriers to isomerization on the C_6H_{10} surface are relatively higher than in the related C_6H_6 system. The more saturated electronic structure of C_6H_{10} appears to play a key role in inhibiting isomerization. Disproportionation to form $C_3H_4 + C_3H_6$ is a minor process, with an upper limit from our work on the ratio of disproportion to recombination of $k_{1b}/k_{1a} \leq 0.03$. Our disproportionation to recombination ratio is consistent with the value 0.008 ± 0.001 reported by James and Kambanis.[21]

The total rate coefficient for the allyl self-reaction at 298 K is $k_1 = (2.7 \pm 0.8) \times 10^{-11}$ cm^3 molecule^{-1} s^{-1}. Our value of k_1 agrees well with those derived from UV kinetic absorption spectroscopy, providing independent support for both these determinations of the rate coefficient and the optical absorption cross-section of allyl radical near 220−223 nm.

Acknowledgment. We thank Mr. Howard Johnsen for excellent technical support. We gratefully acknowledge Dr. Huzeifa Ismail and Prof. William H. Green (Massachusetts Institute of Technology) for communicating their results on the allyl + allyl reaction prior to publication. This work is supported by the Division of Chemical Sciences, Geosciences, and Biosciences, the Office of Basic Energy Sciences, the U.S. Department of Energy. Sandia is a multiprogram laboratory operated by Sandia Corporation, a Lockheed Martin Company, for the National Nuclear Security Administration under Contract DE-AC04-94-AL85000. The Advanced Light Source is supported by the Director, Office of Science, Office of Basic Energy Sciences, Materials Sciences Division, of the U.S. Department of Energy under Contract No. DE-AC02-05CH11231 at Lawrence Berkeley National Laboratory. A.F. acknowledges support of NASA-Planetary Atmospheres Program (award no. NNG05GQ15G).

Supporting Information Available: Figures of total and partial photoionization cross-sections of several C_6H_{10} isomers. This information is available free of charge via the Internet at http://pubs.acs.org.

References and Notes

(1) Cole, J. A.; Bittner, J. D.; Longwell, J. P.; Howard, J. B. *Combust. Flame* **1984**, *56*, 51.

(2) Miller, J. A.; Melius, C. F. *Combust. Flame* **1992**, *91*, 21.

(3) Westmoreland, P. R.; Dean, A. M.; Howard, J. B.; Longwell, J. P. *J. Phys. Chem.* **1989**, *93*, 8171.

(4) Moses, J. I.; Bézard, B.; Lellouch, E.; Gladstone, G. R.; Feuchtgruber, H.; Allen, M. *Icarus* **2000**, *143*, 244.

(5) Moses, J. I.; Lellouch, E.; Bezard, B.; Gladstone, G. R.; Feuchtgruber, H.; Allen, M. *Icarus* **2000**, *145*, 166.

(6) Miller, J. A.; Klippenstein, S. J. *J. Phys. Chem. A* **2003**, *107*, 7783.

(7) DeSain, J. D.; Taatjes, C. A. *J. Phys. Chem. A* **2003**, *107*, 4843.

(8) Fahr, A.; Laufer, A. H.; Tardy, D. C. *J. Phys. Chem. A* **1999**, *103*, 8433.

(9) Howe, P.-T.; Fahr, A. *J. Phys. Chem. A* **2003**, *107*, 9603.

(10) Miller, J. A.; Klippenstein, S. J. *J. Phys. Chem. A* **2001**, *105*, 7254.

(11) Tulloch, J. M.; Macpherron, M. T.; Morgan, C. A.; Pilllng, M. J. *J. Phys. Chem.* **1982**, *86*, 3812.

(12) van den Bergh, H. E.; Callear, A. B. *Trans. Faraday Soc.* **1970**, *66*, 2681.

(13) Nakashima, N.; Yoshihara, K. *Laser Chem.* **1987**, *7*, 177.

(14) Jenkin, M. E.; Murrells, T. P.; Shalliker, S. J.; Hayman, G. D. *J. Chem. Soc., Faraday Trans.* **1993**, *89*, 433.

(15) Boyd, A. A.; Nozière, B.; Lesclaux, R. *J. Chem. Soc., Faraday Trans.* **1996**, *92*, 201.

(16) DeSain, J. D.; Jusinski, L. E.; Taatjes, C. A. *Phys. Chem. Chem. Phys.* **2006**, *8*, 2240.

(17) Ha, T. K.; He, Y.; Pochert, J.; Quack, M.; Ranz, R.; Seyfang, G.; Thanopoulos, I. *Ber. Bunsen-Ges Phys. Chem. Chem. Phys.* **1995**, *99*, 384.

(18) Tonokura, K.; Koshi, M. *J. Phys. Chem. A* **2000**, *104*, 8456.

(19) Ismail, H.; Green, W. H. *Int. J. Chem. Kinet.*, submitted for publication.

(20) Georgievskii, Y.; Miller, J. A.; Klippenstein, S. J. *Phys. Chem. Chem. Phys.* **2007**, *9*, 4259.

(21) James, D. G. L.; Kambanis, S. M. *Trans. Faraday Soc.* **1969**, *65*, 1350.

(22) Mallard, P. J. L. a. W. G. *NIST Chemistry WebBook, NIST Standard Reference Database Number 69*; National Institute of Standards and Technology: Gaithersburg MD, 20899 (http://webbook.nist.gov), June 2005.

(23) Cox, J. D.; Pilcher, G. *Thermochemistry of Organic and Organomettalic Compounds*; Academic Press: London, 1970.

(24) Meloni, G.; Zou, P.; Klippenstein, S. J.; Ahmed, M.; Leone, S. R.; Taatjes, C. A.; Osborn, D. L. *J. Am. Chem. Soc.* **2006**, *128*, 13559.

(25) Goulay, F.; Osborn, D. L.; Taatjes, C. A.; Zou, P.; Meloni, G.; Leone, S. R. *Phys. Chem. Chem. Phys.* **2007**, *9*, 4291.

(26) Meloni, G.; Selby, T. M.; Goulay, F.; Leone, S. R.; Osborn, D. L.; Taatjes, C. A. *J. Am. Chem. Soc.* **2007**, *129*, 14019.

(27) Taatjes, C. A.; Hansen, N.; Osborn, D. L.; Kohse-Höinghaus, K.; Cool, T. A.; Westmoreland, P. R. *Phys. Chem. Chem. Phys.* **2008**, *10*, 20.

(28) Cool, T. A.; Nakajima, K.; Mostefaoui, T. A.; Qi, F.; McIlroy, A.; Westmoreland, P. R.; Law, M. E.; Poisson, L.; Peterka, D. S.; Ahmed, M. *J. Chem. Phys.* **2003**, *119*, 8356.

(29) Robinson, J. C.; Sveum, N. E.; Neumark, D. M. *Chem. Phys. Lett.* **2004**, *383*, 601.

(30) Wolkoff, P.; Holmes, J. L.; Lossing, F. P. *Can. J. Chem.* **1980**, *58*, 251.

(31) Fahr, A.; Laufer, A. H.; Tardy, D. C. *J. Phys. Chem. A* **1999**, *103*, 8433.

(32) Stoliarov, S. I.; Knyazev, V. D.; Slagle, I. R. *J. Phys. Chem. A* **2000**, *104*, 9687.

(33) Thorn, R. P.; Payne, W. A.; Stief, L. J.; Tardy, D. C. *J. Phys. Chem.* **1996**, *100*, 13594.

(34) Ismail, H.; Goldsmith, C. F.; Abel, P. R.; Howe, P.-T.; Fahr, A.; Halpern, J. B.; Jusinski, L. E.; Georgievskii, Y.; Taatjes, C. A.; Green, W. H. *J. Phys. Chem. A.* **2007**, *111*, 6843.

(35) Holbrook, K. A.; Pilling, M. J.; Robertson, S. H. *Unimolecular Reactions*, 2nd ed.; John Wiley & Sons: Chichester, U.K., 1996.

(36) Benson, S. W. *Thermochemical Kinetics*, 2nd ed.; John Wiley and Sons: New York, 1976.

(37) Brown, T. C.; King, K. D.; Nguyen, T. T. *J. Phys. Chem.* **1986**, *90*, 419.

(38) Woodward, R. B.; Hoffmann, R. *Angew. Chem. Int. Ed.* **1969**, *8*, 781.

(39) Houk, K. N.; Li, Y.; Evanseck, J. D. *Angew. Chem., Int. Ed. Engl.* **1992**, *31*, 682.

(40) Ellis, R. J.; Frey, H. M. *J. Chem. Soc.* **1964**, *S*, 5578.

(41) Cool, T. A.; Wang, J.; Nakajima, K.; Taatjes, C. A.; Mcllroy, A. *Int. J. Mass Spectrom.* **2005**, *247*, 18.

(42) Robinson, J. C.; Sveum, N. E.; Neumark, D. M. *J. Chem. Phys.* **2003**, *119*, 5311.

(43) Taatjes, C. A.; Osborn, D. L.; Selby, T. M.; Meloni, G. *J. Phys. Chem. A.* **2008**, *112*, 9336.

(44) Cool, T. A.; McIlroy, A.; Qi, F.; Westmoreland, P. R.; Poisson, L.; Peterka, D. S.; Ahmed, M. *Rev. Sci. Instrum.* **2005**, 76.

(45) Bobeldijk, M.; Zande, W. J. v. d.; Kistemaker, P. G. *Chem. Phys.* **1994**, *179*, 125.

(46) Koizumi, H. *J. Chem. Phys.* **1991**, *95*, 5846.

(47) Shafir, E. V.; Slagle, I. R.; Knyazev, V. A. *J. Phys. Chem. A* **2003**, *107*, 8893.

JP802330K